KeAi

CHINESE ROOTS
GLOBAL IMPACT

Contents lists available at ScienceDirect

Petroleum Science

journal homepage: www.keaipublishing.com/en/journals/petroleum-science



Original Paper

Thickening progression mechanism of silica fume — oil well cement composite system at high temperatures



Hang Zhang ^a, Miao-Miao Hu ^{a, b, c, *}, Peng-Peng Li ^a, Guo-Qing Liu ^a, Qing-Lu Chang ^a, Jie Cao ^a, Ming Liu ^a, Wen-Hua Xu ^d, Xiu-Jian Xia ^d, Jin-Tang Guo ^{a, b, c, **}

- ^a School of Chemical Engineering and Technology, Tianjin University, Tianjin, 300350, China
- ^b Zhejiang Institute of Tianjin University, Shaoxing, 312300, Zhejiang, China
- ^c Haihe Laboratory of Sustainable Chemical Transformations, Tianjin, 300192, China
- ^d CNPC Engineering Technology R&D Company Limited, Beijing, 102206, China

ARTICLE INFO

Article history: Received 18 September 2023 Received in revised form 20 November 2023 Accepted 29 December 2023 Available online 5 January 2024

Edited by Min Li

Keywords:
Silica fume
Oil well cement
Thickening time reversal
Pozzolanic reaction
Adsorptive barrier
CH and C-S-H

ABSTRACT

This work studied the thickening progression mechanism of the silica fume - oil well cement composite system at high temperatures (110-180 °C) in order to provide a theoretical guidance for the rational application of silica fume in the cementing engineering. Results showed that silica fume seldom affected the thickening progression of oil well cement slurry at 110-120 °C, but when temperature reached above 130 °C, it would aggravate the bulging degree of thickening curves and significantly extend the thickening time, meanwhile causing the abnormal "temperature-based thickening time reversal" and "dosage-based thickening time reversal" phenomena in the range of $130-160~^{\circ}\text{C}$ and $170-180~^{\circ}\text{C}$ respectively. At 130-160 °C, the thickening time of oil well cement slurry was mainly associated with the generation rate of calcium hydroxide (CH) crystal. The introduced silica fume would be attracted to the cement minerals' surface that were hydrating to produce CH and agglomerate together to form an "adsorptive barrier" to hinder further hydration of the inner cement minerals. This "adsorptive barrier" effect strengthened with the rising temperature which extended the thickening time and caused the occurrence of the "temperature-based thickening time reversal" phenomenon. At 170-180 °C, the pozzolanic activity of silica fume significantly enhanced and considerable amount of C-S-H was generated, thus the "temperature-based thickening time reversal" vanished and the "dosage-based thickening time reversal" was presented.

© 2024 The Authors. Publishing services by Elsevier B.V. on behalf of KeAi Communications Co. Ltd. This is an open access article under the CC BY-NC-ND license (http://creativecommons.org/licenses/by-nc-nd/4.0/).

1. Introduction

Oil well cement (OWC) is a kind of Portland cement specially used in cementing engineering of oil/gas wells. The application environment of the OWC is usually harsh because many of the remaining oil/gas resources are still buried in deep formations with high temperatures (Guo et al., 2020; Liu et al., 2023). As a kind of well-known functionalized filler, silica fume (SF, also called microsilica (Diamond and Sahu, 2006) with high pozzolanic

reactivity, ultra-fine particle size (0.1–1 μm) (Qin et al., 2021) and high specific surface area (18000 m²/kg) (Inan Sezer, 2012) is widely used in OWC systems (Jupe et al., 2008; Qin et al., 2021) to improve their performances. In recent years, many literatures have reported its effects on the hydration process (Lei et al., 2016; Yang and He, 2021), mechanical strength (Atiş et al., 2005; Chakrabortya and Dutta, 2001; Shannag, 2000), mixing properties (Burroughs et al., 2019; Qian et al., 2008) and rheological behaviors (Burroughs et al., 2019; Vikan and Justnes, 2007) of cementitious composites. In summary, there are three main application values of SF in the OWC system. Firstly, it is helpful in reducing the bleeding of free fluid and improving the suspension of the OWC slurry (Li, 2020). Secondly, it is beneficial to improve the fluid loss control capacity of fluid loss additive by optimizing the particle size distribution of OWC grains via its micro-filling effect to refine the pore structure (Qin et al., 2021; Scheinherrová et al., 2017; Zhang et al.,

^{*} Corresponding author. School of Chemical Engineering and Technology, Tianjin University, Tianjin, 300350, China.

^{**} Corresponding author. Corresponding author. School of Chemical Engineering and Technology, Tianjin University, Tianjin, 300350, China.

E-mail addresses: mmhu1990@tju.edu.cn (M.-M. Hu), jtguo@tju.edu.cn (I.-T. Guo).

2016). Lastly, depending on its "close-packed" effect and pozzolanic effect (Atiş et al., 2005; Chakrabortya and Dutta, 2001; Li et al., 2023a; Shannag, 2000), it can also enhance the mechanical performances of hardened cement at low temperatures (Cheng et al., 2018).

To date, the application of SF in the low temperature (<110 °C) cementing industry is relatively mature based on its stable lowtemperature thickening performance. However, the application environment of the OWC system is gradually developing towards high-temperature and high-pressure (HTHP) formation conditions (>110 °C) (Pernites and Santra, 2016; Qin et al., 2021). This environment tends to cause the unfavorable abnormal thickening phenomena which mainly includes the abnormal gelation and thickening time reversal (TTR) (Chen et al., 2017; Vuk et al., 2000; Zhang et al., 2021). The abnormal gelation is reflected by the occurrence of gelled cement around the stirring shaft which in cementing field would obstruct the narrow annulus area between the metal pipe and the well wall, thus increasing the pumping pressure and even choking the pump in severe cases. The TTR phenomenon includes two situations. The first one is the "temperature-based TTR" (Jiang et al., 2008; Zhang et al., 2021), which refers to the condition that the thickening time (TT) of OWC slurry at higher temperature is longer than that at lower temperature. Under normal conditions, a higher temperature typically accelerates the cement hydration and shortens the TT. However, this adverse phenomenon would cause the cement slurry to gradually set from top to bottom, making the static pressure of the lower unsetting slurry drop and may further trigger annular gas channeling (Guo et al., 2014, 2019a). Moreover, this phenomenon can also lead to uneven hydration of OWC slurry, thus affecting the cementing quality. Another one situation is the "dosage-based TTR", which means that the TT shortens instead of extends with the increasing dosage of additives. This phenomenon is not conducive to the adjustment and regulation of TT. Previous research laid emphasis on the effects of various retarders on the abnormal thickening phenomena. Chen et al. (2017) studied the cause of the abnormal gelation at 120 °C initiated by polycarboxylate retarder, and showed that unproper molecular chain structure of retarder would lead to excessive complexation reaction between -COO-, Ca^{2+} and SiO_4^{4-} to form flocs. Sun et al. (2022) reported that the abnormal gelation caused by tartaric acid at 70 °C was due to the fact that it induced earlier hydration of C₃A and C₄AF before the hydration of other silicate minerals. Guo et al. (2014, 2019a) found that the addition of tartaric acid could avoid the "temperaturebased TTR" of the OWC containing AMPS-IA binary copolymer retarder at 75-85 °C which may be because it reduced the hydration rate difference of C₄AF between 75 and 85 °C. In general, current research about TTR mainly focused on investigating the impact of retarders and there lacks corresponding studies of other commonly used admixtures (such as SF) on the effect of thickening performance of the OWC system so far, which is of practical significance in the field application.

The dynamic thickening progression of OWC is closely related to its hydration rate (Wang et al., 2022b). When the slurry hydrates to a level that completely loses its fluidity, at this point the slurry reaches the set time (the set of OWC slurry under dynamic stirring conditions is so-called thickening). Therefore, we could draw inspiration from the research on the cement hydration involving SF. Jupe et al. (2008) reported for the first time that SF could inhibit the hydration of C_3S in class H OWC at 180 °C and delay the early strength development of the cement, and the reason of this phenomenon was not further analyzed in this paper. Bhattacharya and Harish (2018) reported that the addition of SF could consume the $Ca(OH)_2$ generated from cement hydration at early-curing periods due to its dilution effect and pozzolanic effect, meanwhile retarded

the cement early hydration which was more prominent at higher dosages of SF. It seems contradictory that SF not only promoted the conversion of CH into C-S-H but also delayed the early hydration of cement which was similar to our research results, but the cause for this phenomenon was not expounded in this paper. Lei et al. (2016) and Mitchell et al. (1998) reported the SF could attract each other to form the agglomerates which may become a coat to impede further hydration, and the agglomerates were hard to be broken down by ordinary mixing (Yajun and Cahyadi, 2003). This theory is somewhat convincing, and still needs improvement to explain the discrepant effect of SF on the cement hydration with changing temperature. Meanwhile, there are also some literatures reported that SF promoted cement hydration at low temperatures. Huang and Feldman (1985) and Jeong et al. (2020) found that the SF could accelerate the ordinary Portland cement (OPC) hydration at 20 and 23 °C, respectively. In summary, current literatures studied the effect of SF on the hydration reaction of OPC at different temperatures, to date there still lacks systematic study on the hydration of dynamic thickening progression of OWC at high temperatures.

As a qualified thickening performance is a prerequisite for ensuring the safe application and directly related to the pumping security of the OWC slurry (Guo et al., 2019b), this study aimed at the effect of SF on the dynamic thickening progression of class G OWC slurry at 110–180 °C from the perspective of analyzing the instantaneous hydration circumstance at different curing times using the microstructure characterization techniques (XRD, TG-DTG and ²⁹Si-NMR), and the HTHP consistometer was used to provide the dynamic stirring conditions for OWC slurry curing.

2. Experimental

2.1. Materials

The class G OWC used in this work was purchased from Jiahua Special Cement Co., Ltd (Sichuan, China) and its production date was April 2022. Its chemical and mineral composition was determined by XRF (model S4 Pioneer, Bruker-AXS) and QXRD (model D8-Focus, Bruker AXS, Germany). The QXRD characterization was performed at a scan speed of 3°/min using the corundum as an external standard (Hakamy et al., 2015; Sun et al., 2023b), and then the Rietveld refinement was performed in the Maud software (Zhang et al., 2023). Corresponding XRD pattern and compositions of this OWC are presented in Fig. S1 and Table S1 (see supplementary material, same below), respectively.

Quartz sand (200 mesh), silica fume (SF), retarder (DRH-3L), fluid loss additive (DRF-3L), dispersant (DRS-1S), stabilizer (DRK-3S) and defoamer (DRX-1L) were all supplied by CNPC Engineering Technology R&D Co., Ltd (Beijing, China), the main chemical compositions of these additives are listed in Table S2. In addition, chemical compositions (determined by XRF), XRD patterns and SEM images of the SF and quartz sand (200 mesh) used in this paper are respectively shown in Table S3 and Fig. S2.

2.2. Thickening tests of cement slurry

The thickening test process was based on section 9.3 of API Recommended Practice 10B-2 "Recommended Practice for Testing Well Cements" (API, 2013) conducted in a HTHP consistometer (model TG-8040D10, Shenyang Taige Oil Equipment Co., Ltd, China).

Since the effect of SF on the HTHP thickening performance of OWC system lacks systematic study so far, this work aimed at investigating the effect of SF on the thickening performance at a broad high-temperature range (110–180 $^{\circ}$ C), in order to provide a theoretical guidance for the rational application of SF in the

Table 1The composition and dosage of the cement slurry in this work.

Test temperature, °C	Cement, §	g Quartz sand (200 mesh), % bwoc, same below	SF, %	Retarder, %	Fluid loss additive, %	Dispersant, %	Stabilizer, %	Water, %
110, 120, 130	500.0	35.0	0, 2, 4		4.5	0.8	0.6	53.0
130–180 (tested at 10 °C interval) 500.0	35.0	0, 2, 4		4.5	0.8	0.6	52.0

cementing engineering. The composition of the OWC slurry for all thickening tests was kept consistent except for three dosages' change of SF (0%, 2%, 4% bwoc). Two fixed retarder dosages (1.5% and 2.7% bwoc) were selected to suit for different temperature range. The detailed formulae of the cement slurry systems ($\rho=1.89\pm0.01~g/cm^3)$ in this work are listed in Table 1. For all thickening experiments, the control variate method was used to maintain the comparability of these experiments. Except for the difference in the test temperature, the heating and pressurizing time were set as 60 min and the final pressure was set as 70 MPa which were similar to the actual bottomhole conditions.

What should be clarified is that the thickening time test using the consistometer was a kind of highly reproducible testing method with very small experimental errors and was usually conducted only once in most literatures (Guo et al., 2017; Liu et al., 2015; Lu et al., 2016; Peng et al., 2020; Sun et al., 2022; Zhang et al., 2021). To make the above statement more rigorous, an example of three repeated thickening tests of the OWC slurry was presented in Fig. 1, and the obtained thickening time were 146.5, 147.0 and 144.5 min, respectively. It could be seen that the thickening experiments using the same cement slurry formula had high repeatability (the corresponding calculated standard deviation was 1.08 min and the coefficient of variation was 0.74%), thereby each different thickening experiment was run only once in this paper.

2.3. Analytical methods

In order to study the effect and mechanism of SF on the thickening performance of OWC system at high temperatures, the slurry samples after curing in the HTHP consistometer for different time until final thickening were all collected, freeze-dried, ground into powder and passed through a 200-mesh sieve for next physiochemical analyses. The XRD (model D8-Focus, Bruker AXS, Germany) tests were carried out from 5° to 70° at a scan speed of 7°/min for cement samples. Secondly, the TG analysis (model TG 209F3, NETZSCH-Gerätebau GmbH, Germany) was performed under N2 atmosphere and the sample was heated up from 35 to 600 °C at a rate of 10 °C/min. Finally, the solid $^{29}\mathrm{Si}$ NMR (model JNM ECZ600R, JEOL, Japan) was conducted to analyze the Si environment in the cement samples and the MestReNova software was used to process the spectra. The schematic diagram of the experimental method in this work is shown in Fig. 2.

3. Results and discussion

3.1. Effect of SF on the thickening performance of OWC slurry at 110–180 $^{\circ}\text{C}$

The thickening test is an experimental method to simulate the pumping operations of OWC slurry system in laboratory (Wang et al., 2022a). It can not only reflect the thickening time (TT), but also evaluate whether the abnormal phenomena (bulge and high initial consistency) of cement slurry occurs during the pumping operations by observing the thickening curves.

3.1.1. Thickening curve

We carried out the thickening experiments of the OWC slurry with 0%, 2% and 4% bwoc SF at 110–180 °C under proper retarder dosages and 70 MPa. For clear comparison, the thickening curves of 0% and 4% SF are displayed in Fig. 3, as the curve shapes of 2% SF are similar to 4% SF and the difference is only the TT. In addition, we offset-plotted the thickening curves within initial 100 min of each sample in Fig. 3 ((b), (d), and (f)) on the same *Y*-axis scale to distinguish them clearly.

As could be seen, all the thickening curves without SF were

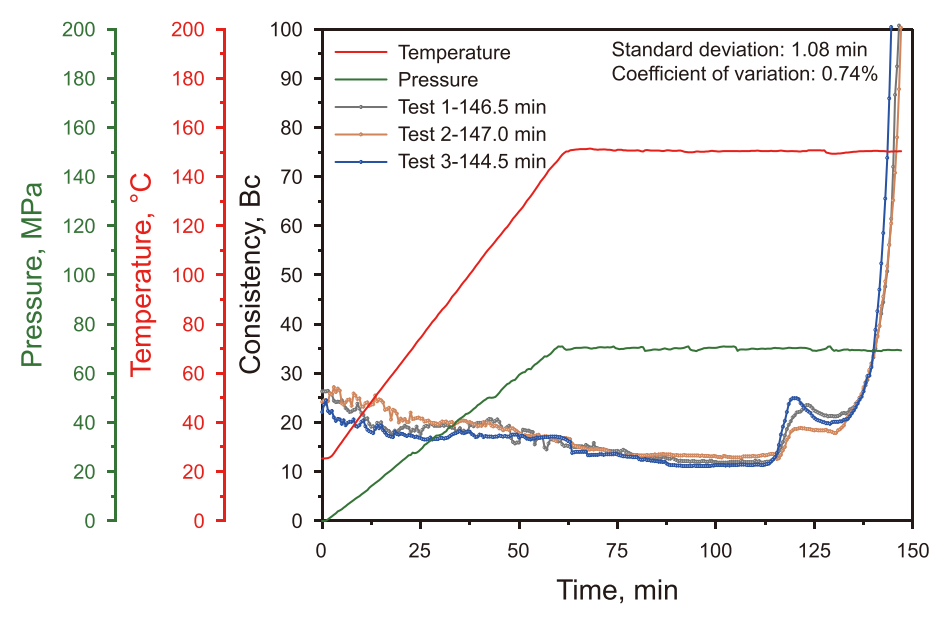


Fig. 1. Three repeated thickening tests of the OWC slurry without SF at 150 $^{\circ}$ C/70 MPa.

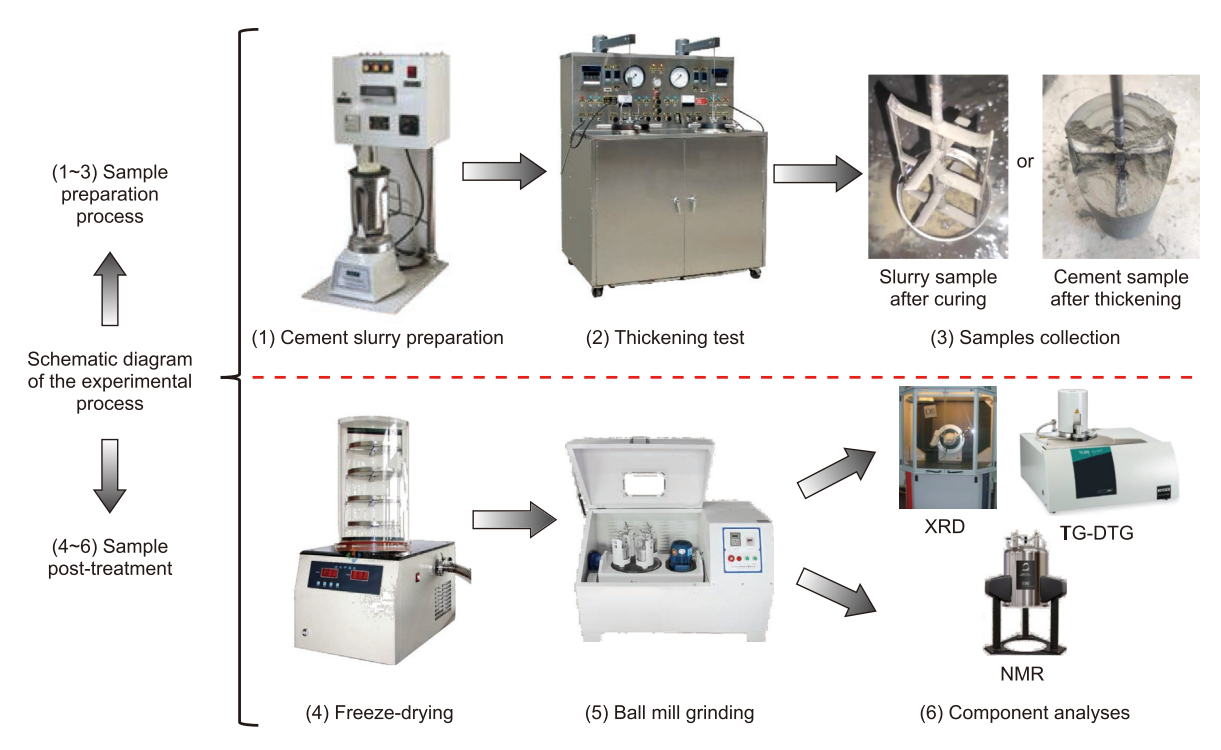


Fig. 2. Schematic diagram of the experimental method in this work.

relatively smooth and the addition of SF hardly affected the line shape at 110 and 120 °C. However, the addition of SF incurred the bulge phenomenon at 130-180 °C when the thickening process approached to 50–60 min (near the end of heat-up). Within several minutes during the occurrence of the bulge phenomenon, the thickening curve presented a sharply increased consistency which might choke the pump in the field and lead to cementing accident (Sun et al., 2022), thus we have repeated the thickening experiments containing SF in Fig. 3(c) and (e) and stopped them in advance (curing 30 min after reaching target temperature) to observe whether the stirring shaft was wrapped by gelatinous cement. Different from the common abnormal gelatinous cement that would stay on the stirring shaft (Chen et al., 2017; Zhang et al., 2021), we found that the stirring shafts of slurries with 4% SF were all very clean (no gelatinous cement remaining winding on the stirring shaft) despite experiencing such large bulges, which was due to the fact that the introduction of SF caused an unfirm abnormal gelation followed by the disintegration of this gelatinous cement. Since the OWC slurry without SF did not present obvious bulging phenomenon, we could confirm that the SF must be involved in the bulging reaction, and then the hydration rate of cement was changed (manifested as the TT was changed). In next sections, this paper would further analyze the reason of SF retarding the thickening progression above 130 °C.

3.1.2. Thickening time

Normally, the hydration of OWC slurry accelerates with the increase of temperature and the TT shortens correspondingly, which is a favorable phenomenon for cementing. Therefore, it is necessary to study the tendency of TT evolution of "SF-OWC" system at different temperatures. Fig. 4(a)—(b) shows the effect of SF (0%, 2%, 4% bwoc) on the TT of the cement slurry in the range of $110-180\,^{\circ}$ C. From Fig. 4(a) we could see that in the range of $110-130\,^{\circ}$ C, the TT was hardly affected (slightly shortened or basically stable) after the addition of SF. In contrast, from Fig. 4(b) we found that when the

temperature exceeded 130 °C, only the addition of 2% bwoc SF significantly prolonged the TT at 140–180 °C. For instances, the TT of 2% bwoc SF was 225.5 min (96.6%) longer than 0% bwoc SF at 140 °C and 211.5 min (235.3%) longer at 150 °C, and this retarding effect for 4% bwoc SF was even more severe. The reason why SF has strong retardation at 140–180 °C was the first issue that would be studied in this article (in the next section).

Another finding in Fig. 4(b) was that there were two different tendencies in the temperature range of 130-160 °C and 170-180 °C. For the former, the TT extension degree after introducing SF gradually increased as the temperature rose from 130 to 160 °C. Specifically, taking 4% bwoc SF as an example, the TT at 140 °C (488.5 min) was 11.5% longer than 130 °C (438 min), 150 °C (696 min) was 42.5% longer than 140 °C (488.5 min) and 160 °C (>960 min) was 37.9% longer than 150 °C (696 min). This abnormal behavior of "temperature-based TTR" endangers cementing operations (Sun et al., 2023a) (as mentioned in the introduction section), thus the introduction of SF into the OWC slurry system should be avoided when the cementing temperature comprises 130–160 °C. For the latter, "temperature-based TTR" phenomenon did not occur at 170-180 °C. Instead, the retarding effect of SF weakened with the increase of its dosage and the "dosage-based TTR" phenomenon occurred. Specifically speaking, the TT of 4% bwoc SF at 170 and 180 °C was respectively 29.8% and 53.1% shorter than 2% bowc SF. Although this phenomenon has no direct harm to cementing, it is unfavorable for the TT regulation. We need to work out why SF would exhibit different retarding behaviors in different temperature ranges of 130–160 $^{\circ}\text{C}$ and 170–180 $^{\circ}\text{C}$ (in the next section).

3.2. Study of SF initiating "temperature-based TTR" of the OWC slurry at 130–150 $^{\circ}\text{C}$

In order to investigate why SF was able to retard the thickening progression when temperature exceeded 130 °C and caused

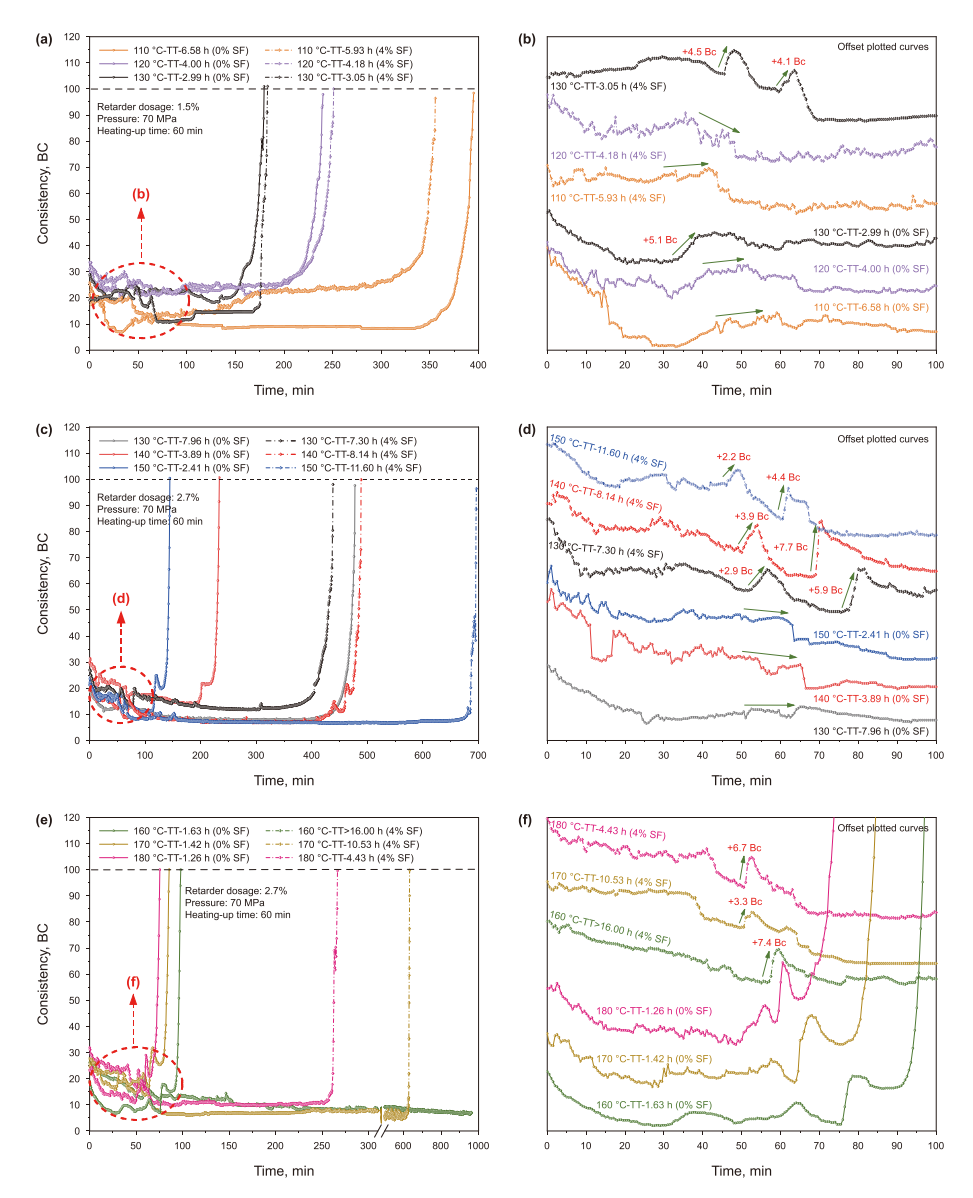


Fig. 3. The thickening curves of OWC cement slurry without/with 4% bwoc SF at (a)—(b), 110—130 °C; (c)—(d), 130—150 °C and (e)—(f), 160—180 °C (experimental pressure: 70 MPa). Note 1: The curves in Fig. 3 ((b), (d) and (f)) were separately arranged on the same Y-axis scale for clearer presentation. Note 2: In this paper, "TT" represents thickening time and "CT" represents curing time.

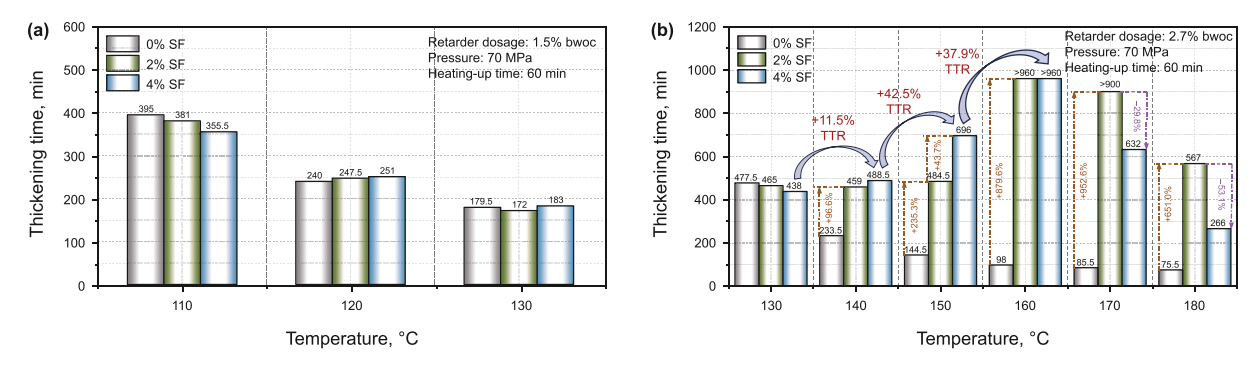


Fig. 4. Effect of SF on the thickening time of the OWC slurry: (a) 110–130 °C/0 MPa/1.5% retarder and (b) 130 °C-180 °C/70 MPa/2.7% retarder.

"temperature-based TTR" at 130-160 °C, the OWC system with 0%/4% bwoc SF and 2.7% retarder in Fig. 4 was selected to analyze the

reason. Specifically speaking, three temperature points (130, 140 and 150 $^{\circ}$ C) were analyzed in detail, as the TT of the slurry with 4%

bwoc SF at 160 °C was too long to thicken beyond 16 h which was far more than the suitable TT required for the cementing operation. In addition, since the TT of the OWC slurry with 0% SF at 150 °C was 144.5 min (2.41 h that was close to 2.50 h) and for comparative study, we additionally had all the slurries with 0% and 4% bwoc SF respectively cured at 130, 140 and 150 °C/70 MPa in the HTHP consistometer for 2.5, 4.5 h, etc., until reaching final TT (Repeated the same thickening experiment and stopped at different curing times to obtain the cement samples). The post-treatment method of all the collected cement slurry or thickened cement samples followed the introduction of section 2.3.

3.2.1. Test and characterization results

3.2.1.1. XRD spectra. The XRD spectra of the cement slurry without SF curing from 130 to 150 °C and 70 MPa for different times are presented in Fig. 5. As could be seen, there was no obvious diffraction peak of calcium hydroxide (CH) in the "130 °C-CT-2.50 h (0% SF)" curve but it gradually enhanced with the extension of curing time (CT), and much CH had been accumulated when the cement slurry reached final thickening. Hence, even though the quartz sand (200 mesh) was added, its pozzolanic effect was not quickly enough to significantly inhibit the formation of CH during the thickening progression of the cement slurry. When the curing temperature increased to 140 and 150 °C, the appearance time of the CH diffraction peak was greatly advanced, indicating that rising temperature led to the acceleration of the CH crystal generation, meanwhile the TT of the cement slurry was also shortened accordingly. In conclusion, the TT of OWC slurry was associated with the generation rate of the CH crystal, the faster production rate of the CH corresponded to the shorter TT. Moreover, we observed that a certain amount of α-C₂SH crystal was produced after 140 and 150 °C thickening, which was a high-permeability and lowstrength hydration product (Krakowiak et al., 2015; Pernites and Santra, 2016; Sun et al., 2023b) and this hydration product was not found in the "130 °C-TT-7.96 h (0% SF)" curve.

Fig. 6 exhibits the XRD spectra of the cement slurry with 4% bwoc SF curing from 130 to 150 $^{\circ}$ C for different times. In Fig. 6(a), the CH peak was absent when curing at 130 $^{\circ}$ C for 4.50 h but it

presented within 7.30 h. Since the 130 °C was a temperature boundary, such a slight delay of CH formation was not sufficient to cause a considerable impact on TT of 130 °C. However, as the curing temperature increased to 140 and 150 °C, the formation time of CH was more significantly delayed. As could be seen, the cement slurry would reach final thickening at 3.89 h at 140 °C (0% SF) accompanied by the formation of a large amount of CH. For comparison, even no CH peak at 18.1° was found after curing at 140 °C for 4.50 h when 4% SF was added. Likewise, this phenomenon was more pronounced at 150 °C and even when the slurry was cured for 8.14 h, there was still no CH peak appearing.

According to the phenomena above, we speculated that there were two possible reasons deferring the thickening progression of cement slurry: (1) the SF with higher pozzolanic activity than quartz sand as curing temperature rose from 130 to 150 °C could retard the generation rate of CH crystal; (2) Previous reports (Bhattacharya and Harish, 2018; Jupe et al., 2008; Mitchell et al., 1998) showed that the agglomeration (low dispersity) behavior of SF in the cement slurry would form a coating on the cement surface to further retard the early hydration of cement, and this behavior aggravated with the increase of SF dosage (Bhattacharya and Harish, 2018). Driven by the pozzolanic reaction, SF in the form of agglomerates was attracted by Ca²⁺ (came from CH) in alkaline pore solution (Greenberg, 1956; Lei et al., 2016) and covered the surface of cement minerals, forming an "adsorptive barrier" to further inhibit the early hydration of cement. Due to the relatively slow generation rate of CH within 130 °C, the "adsorptive barrier" layer was not firm enough to exhibit significant retarding effect. In contrast, when the temperature increased from 130 to 150 °C, the cement tended to accelerate the generation of CH (provided Ca²⁺ faster), which consumed themselves to attract more SF and strengthen the "adsorptive barrier" effect, making a firmer and denser blocking layer to retard thickening progression (presented as the "temperature-based TTR" phenomenon). In addition, compared with the "130 °C-TT-7.96 h (0% SF)" in Fig. 5(a), the diffraction peak of α-C₂SH crystal was appeared in the "130 °C-TT-7.30 h (4% SF)" curve in Fig. 6(a), indicating that the addition of SF promoted the generation of α -C₂SH crystal in the thickening

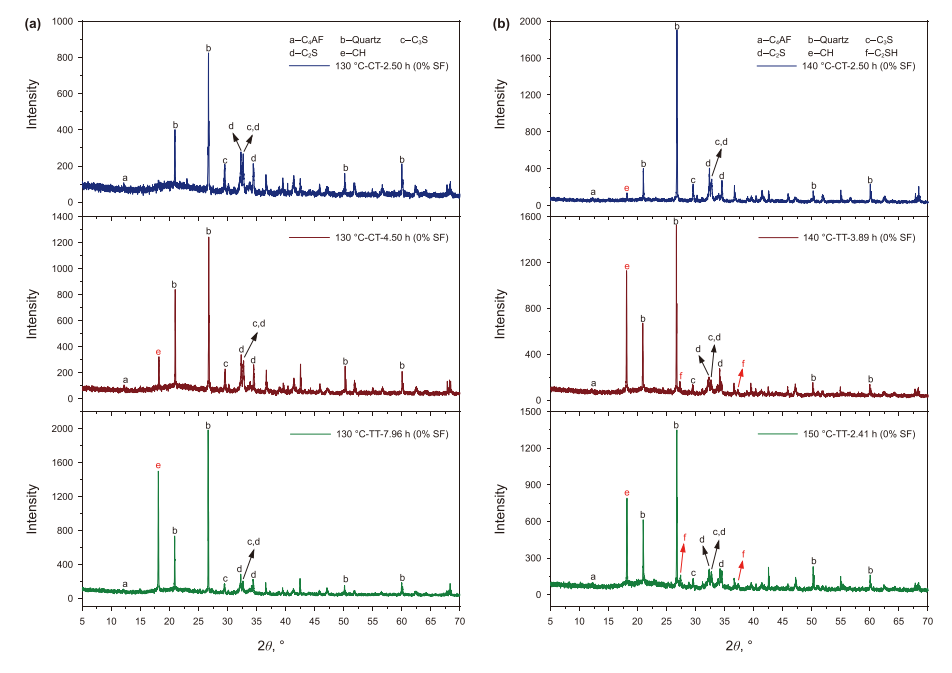


Fig. 5. XRD spectra of the cement slurry without SF curing from 130 to 150 °C and 70 MPa for different times.

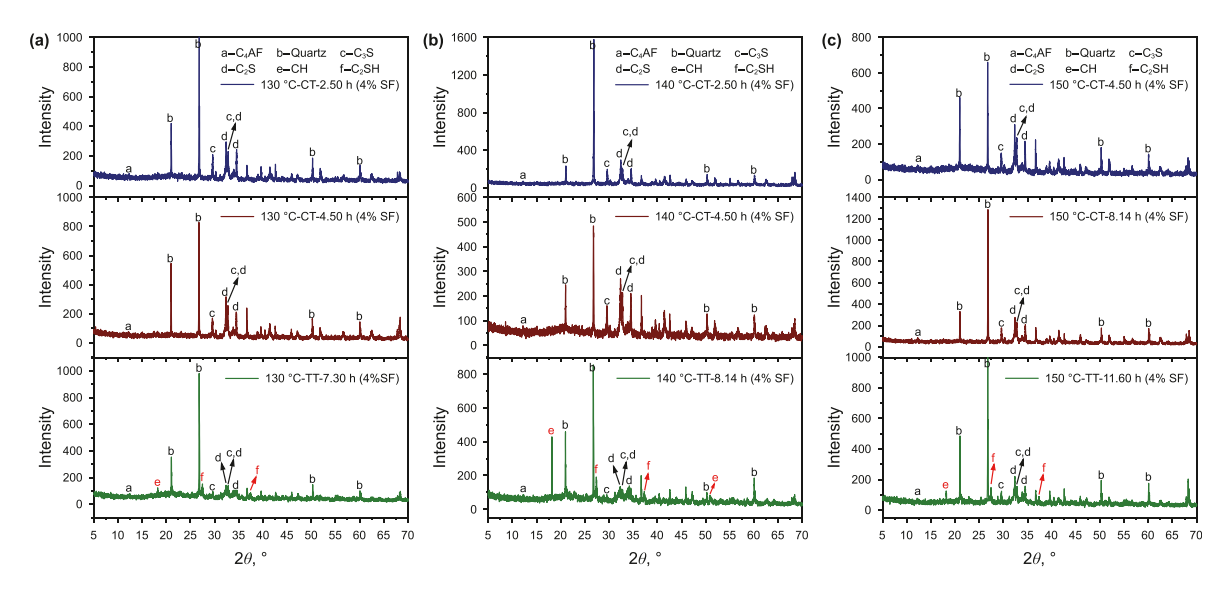


Fig. 6. XRD spectra of the cement slurry with 4% bwoc SF curing from 130 to 150 °C and 70 MPa for different times.

process of the cement slurry at 130 $^{\circ}\text{C}\text{,}$ which was also an unfavorable phenomenon.

3.2.1.2. TG-DTG analyses. To further detect the content evolution of the CH crystals generated by hydration during the curing process of cement slurry, we utilized the TG-DTG method (Fig. 7) to quantitatively determine the content of CH in each cement sample based on the characteristic of CH which gradually decomposed into CaO and free water when heated to near 400 °C (Hakamy et al., 2015; Liu et al., 2021) (Eq. (1)).

$$m_{\rm CH} = \Delta m \frac{M_{\rm CH}}{M_{\rm H_2O}} \tag{1}$$

Wherein $m_{\rm CH}$ represents the mass fraction of CH in the sample, wt %; Δm represents the determined mass loss among 380–450 °C, wt % (Li et al., 2022; Liu et al., 2021; Romano et al., 2019); $M_{\rm CH}$ and $M_{\rm H_2O}$ represent the molar mass of CH and H₂O, respectively.

It should be clarified that the TG curves of thickened cement samples (solid curves) generally have more weight loss than unset cement slurry samples (dash curves). This phenomenon might be owing to the degradation of mineral oil inevitably introduced by the HTHP consistometer, which could not be removed in the hardened cement samples. In contrast, part of the mineral oil in the unset cement slurry samples could float to the surface in the standing freezing process which could be removed so that their weight losses were relatively low. We could see that the DTG peak of CH near 400 °C was highly significant so that the decomposition of trace mineral oil among 380–450 °C would not cause too much error for the determination of CH content.

Fig. 8 shows the evolution of the CH content in the cement slurry during the thickening progression at 130–150 °C. Combining the TG results with XRD patterns, we can obtain that an observable diffraction peak at 18.1° requires the content of CH is greater than 2 wt%. When the cement slurries without SF were all cured at 130–150 °C for 2.50 h, the CH content increased with the rise of

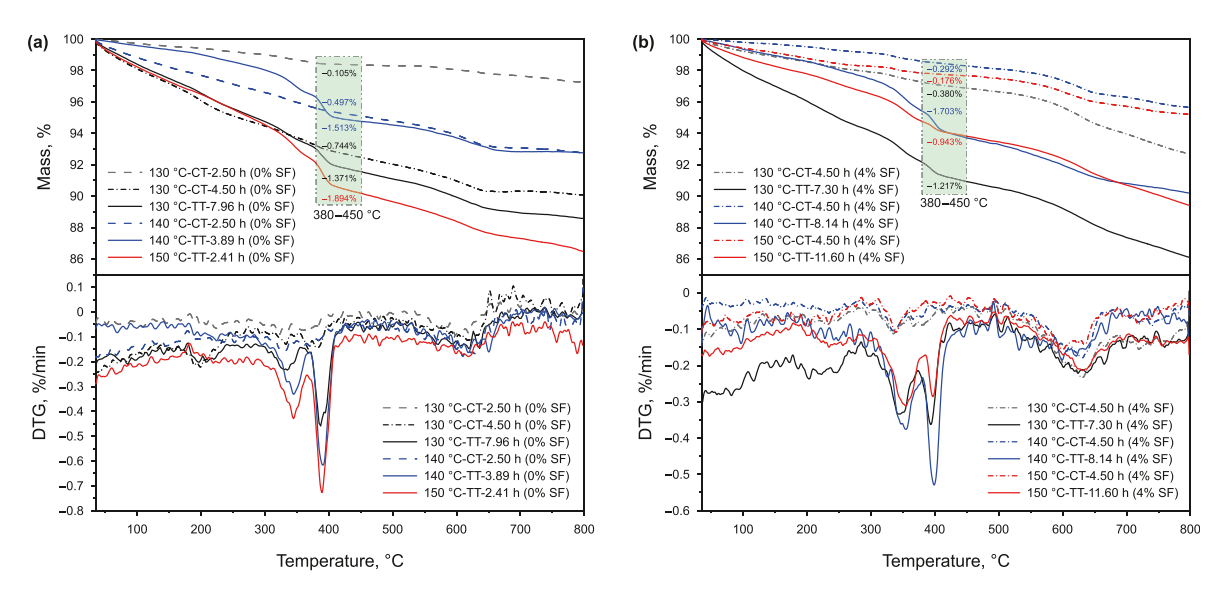


Fig. 7. TG-DTG curves of the cement samples (a) without SF and (b) with 4% bowc SF curing at 130–150 °C and 70 MPa for different times.

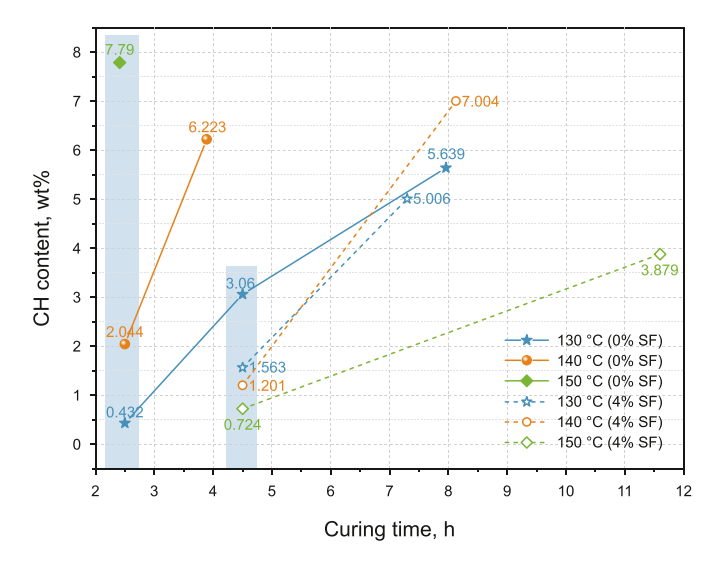


Fig. 8. Evolution of the CH content in the cement samples without/with 4% bowc SF curing at $130-150~^{\circ}\text{C}$ and 70~MPa for different times determined by TG method.

temperature, correspondingly the TT presented as an opposite trend. Instead, as for the cement slurries with 4% bwoc SF cured at 130–150 °C for 4.50 h, the CH content decreased with the rising temperature. This indicated that the consumption of the generated CH by SF became more pronounced as the temperature rose.

3.2.1.3. ²⁹Si NMR spectra. Calcium silicate hydrate (C-S-H) is another kind of common hydration product of cement which usually has an amorphous structure (Pang et al., 2022) and thus hard to be analyzed by XRD patterns. ²⁹Si NMR is a sensitive method to determine the microstructure of C-S-H in hydrated cement samples. Solid ²⁹Si NMR spectra of cement slurry curing at 130–150 °C for different times are shown in Fig. 9. It could be seen that the cement slurry before/at final thickening at 130-150 °C contained a large amount of unhydrated minerals (C₃S, C₂S and C₄AF). Apart from a negligible Q¹ peak was observed at the 150 °C-TT-11.60 h (4%) SF) curve, there were almost only Q^0 (unhydrated C_3S and C_2S) and Q⁴ (SiO₂) (Kurumisawa et al., 2013; Sharma et al., 2019) peaks showed in other curves meanwhile all the characteristic peaks of C-S-H (Q^1-Q^3) (Le Saout et al., 2006) were absent. This result indicated that the cement slurry before or at the final thickening (100 Bc) at 130–150 °C only produced negligible amount of C–S–H which was not enough to be detected by ²⁹Si NMR spectra.

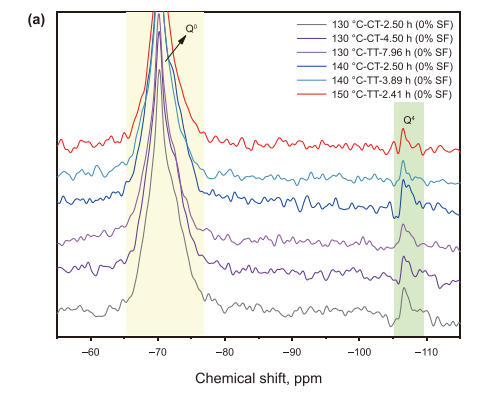
As presented in the range of 130-150 °C by the ²⁹Si NMR

spectra, the pozzolanic reaction between SF and CH only produced negligible amount of C–S–H which was too low to exert considerable influence on the thickening progression. Combined with the XRD and ^{29}Si NMR test results, we concluded that the generation rate of the CH crystal was the major role controlling the TT of 130–150 °C. Hence, the macroscopically displayed retarding degree of the generation of CH by SF enhanced as the temperature rose from 130 to 150 °C which was responsible for the prolongation of TT and the occurrence of the "temperature-based TTR" phenomenon.

3.2.2. Mechanism analyses

Through the research above, we summarized the test conclusions and proposed corresponding analyses from the microscopic perspective to explain why the introduction of SF would cause the "temperature-based TTR" in the range of 130-160 °C.

- (1) Test conclusions: The thickening process of the OWC slurry within this temperature range would not generate a significant amount of C–S–H, so that the TT was mainly associated with the generation rate of the CH crystal. As for the cement slurry without SF, the temperature rise led to the acceleration of the CH crystal generation, and the TT was shortened accordingly. After the introduction of SF, the macroscopic test results presented a slow-down of the CH generation rate above 130 °C and led to an extension of the TT. Such a delay effect on the CH generation gradually increased with the temperature rising from 130 to 160 °C, thereby the "temperature-based TTR" phenomenon occurred.
- (2) Microscopic analyses: According to the test results above, we proposed an "adsorptive barrier" theory to explain these experimental findings, and the schematic diagram of the interaction mechanism of SF-OWC system at 130-160 °C is shown in Fig. 10. We inferred that the cement slurry containing SF would still hydrate to produce CH normally as the same as the cement slurry without SF. The difference lay in that the generated Ca²⁺ on the cement mineral surface would attract SF particles (Lei et al., 2016) (based on the weak acid role of SF ($K_1 = 10^{-9.8}$) (Greenberg, 1956; Lei et al., 2016) in the alkaline environment and immediately consumed themselves into the pozzolanic reaction, so that the generation of CH appeared to be "inhibited". Such a behavior of "SF particles attracted Ca²⁺" made the SF in the form of agglomerates cover the cement minerals that were hydrating to produce CH, forming an "adsorptive barrier" to hinder their further hydration. As the cement slurry tended to accelerate the generation of CH (providing Ca²⁺ faster) when the



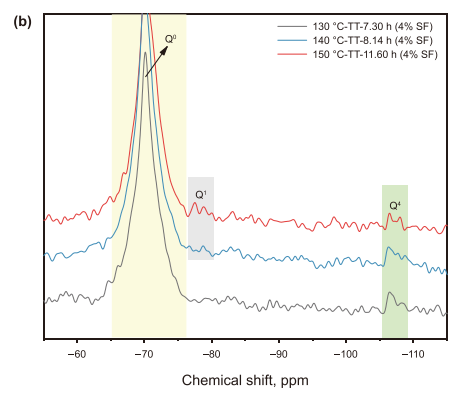


Fig. 9. Solid ²⁹Si NMR spectra of the cement slurry (a) without SF and (b) with 4% bwoc SF curing at 130–150 °C and 70 MPa for different times.

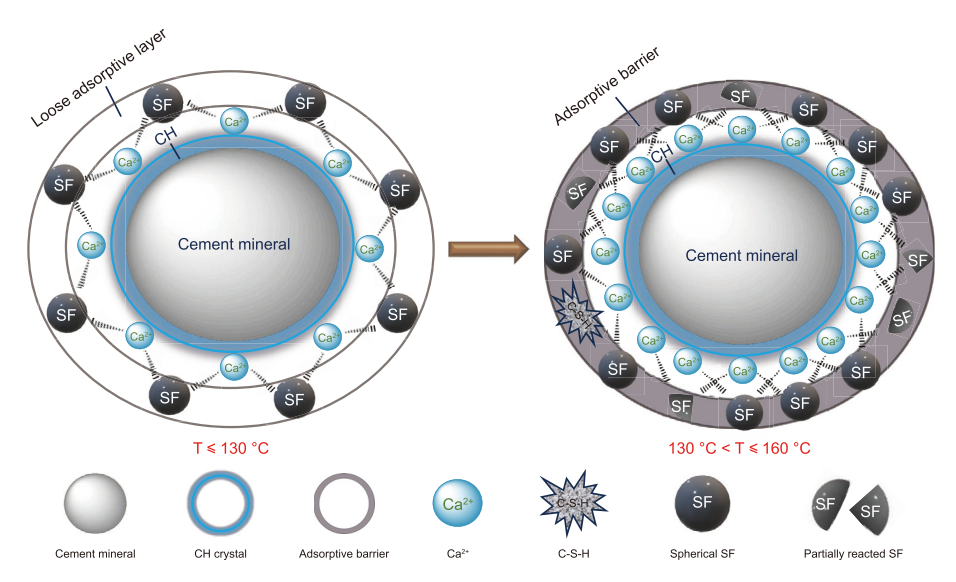


Fig. 10. Schematic diagram of SF initiating "temperature-based TTR" from 130 to 160 °C.

temperature rose from 130 to 160 °C, the behavior of "SF particles attracted Ca²⁺" and consumed CH would become more significant. This process made the adsorptive layer transform from a "loose adsorptive layer" at 130 °C to a firmer and denser "adsorptive barrier" above 130 °C to retard the thickening progression of the inner cement minerals, and thus resulting in the occurrence of the "temperature-based TTR" phenomenon.

What is worth pointing out in advance here is that the "temperature-based TTR" phenomenon would disappear when temperature reached above 160 °C. This is because the pozzolanic activities of SF and quartz sand would all further enhance as the temperature increased from 160 to 180 °C. As a result, considerable amount of C—S—H was generated to promote the shortening of the TT, so that the "temperature-based TTR" phenomenon vanished (but compared to the cement slurry without SF, the "adsorptive barrier" effect would still make the TT extend).

3.3. Study of SF initiating "dosage-based TTR" of the OWC slurry at 180 $^{\circ}C$

To investigate why SF initiated "dosage-based TTR" when temperature reached 170 °C and above which was different from the situation of 130–160 °C, the OWC system with 0%/2%/4% bowc SF and 2.7% bwoc retarder at 180 °C in Fig. 6 was selected to analyze the reason. The OWC slurries with 0%/2%/4% bwoc SF were separately cured at 180 °C/70 MPa for different times until full thickening to collect the cement slurry or thickened cement samples. These samples were all post-treated in the same method described in Section 2.3.

3.3.1. Test and characterization results

3.3.1.1. XRD spectra. The XRD spectra of cement samples with 0–4% bwoc SF curing at 180 °C for different times are displayed in Fig. 11. As was shown, the cement slurry without SF quickly thickened at 180 °C (1.26 h) and produces a large amount of CH and α -C₂SH crystals ("180 °C-TT-1.26 h (0% SF)" curve); On this basis, the TT of the cement slurry was significantly prolonged after introducing 2% or 4% SF because of the "adsorptive barrier" effect, but the "dosage-based TTR" phenomenon was presented which signified that the TT shortened as the dosage of SF increased. Unlike the

results of 130-150 °C (Fig. 6 in Section 3.2.1), there were no CH signals detected in the cement samples containing SF curing at 180 °C even after final thickening. This phenomenon indicated that the pozzolanic activity and "adsorptive barrier" effect of SF were further stimulated at 180 °C (the faster the cement slurry tended to generate CH, the easier the Ca²⁺ tended to attract SF particles to its surface through consuming themselves into the pozzolanic reaction), finally making the test result presented as the generation of CH was almost completely consumed. This process created a strong "adsorptive barrier" to delay the thickening progression and thus extended the TT compared with the cement slurry without SF. Furthermore, we could see that the cement slurry containing SF at 180 °C could also finish thickening even if no considerable amount of CH crystals were generated. Therefore, different from the laws obtained in the range of 130–150 °C in Section 3.2, the generation rate of CH crystals at 180 °C was no longer the single factor controlling the TT of cement slurry. We could also notice that the diffraction peak of α -C₂SH in the samples with SF disappeared, which may be due to SF promoted the transformation of α -C₂SH crystal into amorphous phase at 180 °C.

3.3.1.2. TG-DTG analyses. Fig. 12 shows the TG-DTG curves of the cement samples with 0–4% bwoc SF after curing for different times at 180 °C/70 MPa. It could be seen that the black DTG curve of "180 °C-TT-1.26 h (0% SF)" exhibited a strong CH weight loss peak near 400 °C (Romano et al., 2019) and its content was calculated to be 8.079 wt%. In contrast, there was no peak appeared on other curves at the same position, indicating that the CH content in the samples containing SF were negligible. This result was consistent with the XRD test. In addition, since the amount of C–S–H phase contained in these samples was relatively small (determined by $^{29}\mathrm{Si}$ NMR in the next section), the removable bound water was even less and thus slight DTG peaks in the range of 100–200 °C (Kök, 2013) were observed.

3.3.1.3. 29 Si NMR spectra. The solid 29 Si NMR spectra of the cement samples containing 0–4% bwoc SF after curing at 180 °C/70 MPa for different times are shown in Fig. 13. After the baseline correction of each curve through spline function, we could quantitatively calculate the relative content of Q^1-Q^4 structure in each sample using the area integration method (Li et al., 2023b; Mendes et al., 2011), Corresponding results are shown in Table 2. An example of

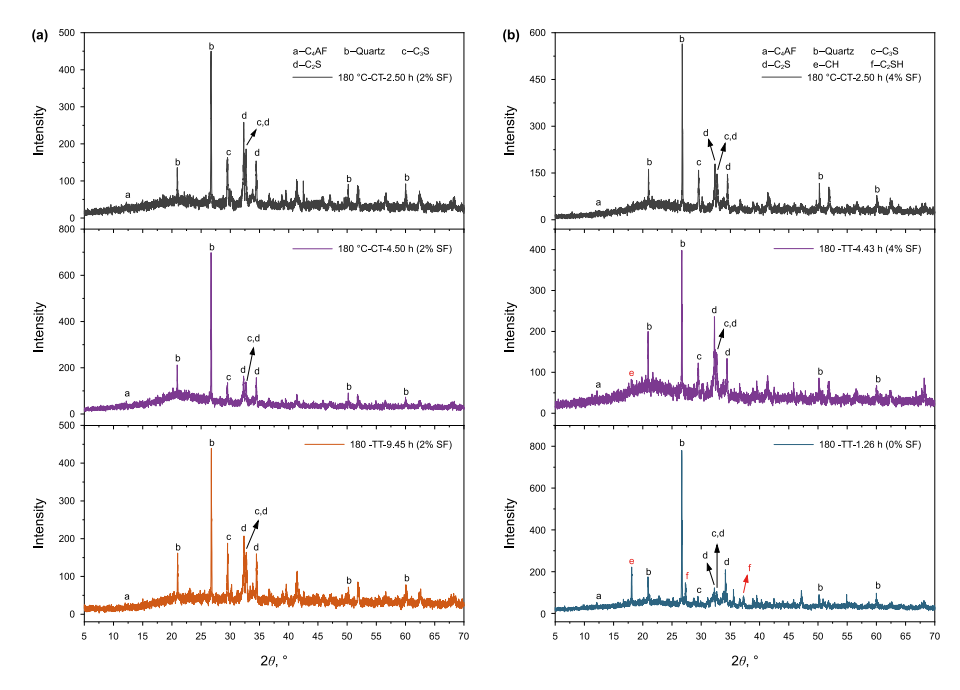


Fig. 11. XRD spectra of the cement slurry with 0%/2%/4% bwoc SF curing at 180 °C/70 MPa for different times.

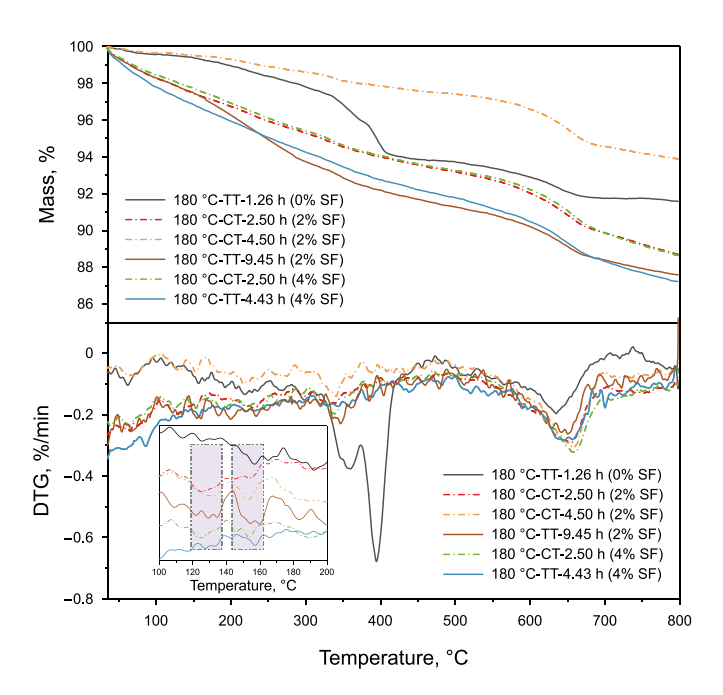


Fig. 12. TG-DTG curves of the cement slurry with 0-4% bowc SF curing at 180 $^{\circ}$ C/70 MPa for different times. (Inset: separately arranged and partial enlarged DTG curves.)

the baseline correction and the integration is presented in Fig. 13(b), and the processing results of other samples are shown in Fig. S3. It could be seen that the pozzolanic activity of 200 mesh quartz sand and SF was all significantly stimulated at 180 °C. At this point, the TT of the cement slurry was jointly controlled both by the generation rate of CH and C–S–H. Since the generated C–S–H has a considerable content, its contribution to thickening could not be ignored. The cement slurry without SF rapidly thickened at 1.26 h (accompanied by the $\rm Q^0$ content rapidly decreased to 85.49 wt%) and produced a large amount of CH (8.08 wt%) and C–S–H

(11.05 wt%). Compared with the absence of SF, the introduction of SF displayed a simultaneous inhibition of the generation of CH (presented in XRD spectra) and C-S-H (presented as the decline of Q^0 and the generation of Q^1-Q^2 were all slowed down) and prolonged the TT. There were two factors need to be considered: (1) Driven by the pozzolanic reaction, the agglomerated spherical SF or partially reacted SF would be adsorbed onto the surface of the cement minerals that were hydrating to produce CH, exerting the "adsorptive barrier" effect to hinder its further hydration and thus synchronously inhibit the generation of CH and C-S-H. (2) The enhanced pozzolanic activity of SF at 180 °C would convert part of SF particles in the "adsorptive barrier" into C-S-H whose generation had the effect of shortening the TT. According to the results from Table 2, we could conclude that the "adsorptive barrier" effect brought by SF still played a dominant role in prolonging TT compared with the absence of SF. When comparing different SF dosages with each other, under the premise of both the existence of "adsorptive barrier", the increase of SF dosage from 2% bwoc to 4% bowc promoted the efficiency of pozzolanic reaction and accelerated the generation of C-S-H since the concentration of SF was increased, so that the TT was shortened with the increase of SF dosage and presented the "dosage-based TTR" phenomenon.

3.3.2. Mechanism analyses

In this section, 180 °C was selected to analyze why SF would cause the "dosage-based TTR" at/above 170 °C. According to the obtained test results, corresponding mechanism was proposed.

(1) Test conclusions: Different from the thickening laws presented in the range of 130–160 °C, the pozzolanic activity of the quartz sand and SF were all significantly stimulated above 170 °C, and the TT of the cement slurry was jointly controlled by the generation rate of CH and C–S–H. The cement slurry without SF finished thickening rapidly along with the synchronous and massive generation of CH and C–S–H within a short time. Compared with the cement slurry without SF, the addition of 2–4% bwoc SF induced a

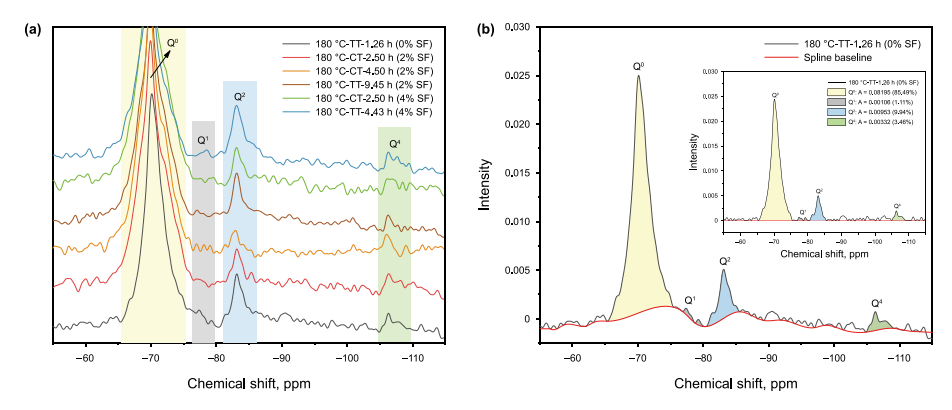


Fig. 13. (a) Solid ²⁹Si NMR spectra of the cement slurry with 0–4% bwoc SF curing at 180 °C/70 MPa for different times. (b) An integration processing example of Q species using spline as baseline (The processing results of other samples are shown in Fig. S3).

Table 2Evolution of the Q species content in the cement samples with 0–4% bowc SF curing at 180 °C/70 MPa for different times determined by²⁹Si NMR.

Cement samples	Relative conte	nt of Q species, wt%	$C-S-H~(Q^1+Q^2)$ content, wt%		
	Q_0	Q ¹	Q^2	Q ⁴	
180 °C-TT-1.26 h (0% SF)	85.49	1.11	9.94	3.46	11.05
180 °C-CT-2.50 h (2% SF)	91.82	0.61	4.22	3.34	4.83
180 °C-CT-4.50 h (2% SF)	91.77	0.61	4.71	2.91	5.32
180 °C-TT-9.45 h (2% SF)	87.58	0.67	9.09	2.66	9.76
180 °C-CT-2.50 h (4% SF)	91.31	0.90	5.34	2.45	6.24
180 °C-TT-4.43 h (4% SF)	85.86	1.13	10.96	2.04	12.09

complete "inhibition" of the CH generation and a delay of the C-S-H generation, resulting in a significant extension of the TT. When comparing different dosages of SF, the increase of SF dosages accelerated the generation of C-S-H and shortened the TT, thus showing the "dosage-based TTR" phenomenon.

(2) Microscopic analyses: The schematic diagram of the disappearance of "temperature-based TTR" and the occurrence of "dosage-based TTR" above 160 °C is shown in Fig. 14. As temperature reached above 160 °C, the pozzolanic reaction between SF and CH enhanced and this process made many SF particles convert into C–S–H. Therefore, the composition

difference of the "adsorptive barrier" between the ranges of 170–180 °C and 130–160 °C lay in that the former consisted of more partially reacted irregular SF and amorphous C–S–H than the latter instead of intact SF particles. Although the composition of the "adsorptive barrier" changed to the combination of SF and some C–S–H, the existence of "adsorptive barrier" still played a dominant role in prolonging TT compared with the absence of SF. When comparing different dosages of SF, the generated CH was completely consumed and the TT was controlled only by the generation rate of C–S–H. The increase of SF dosages increased the

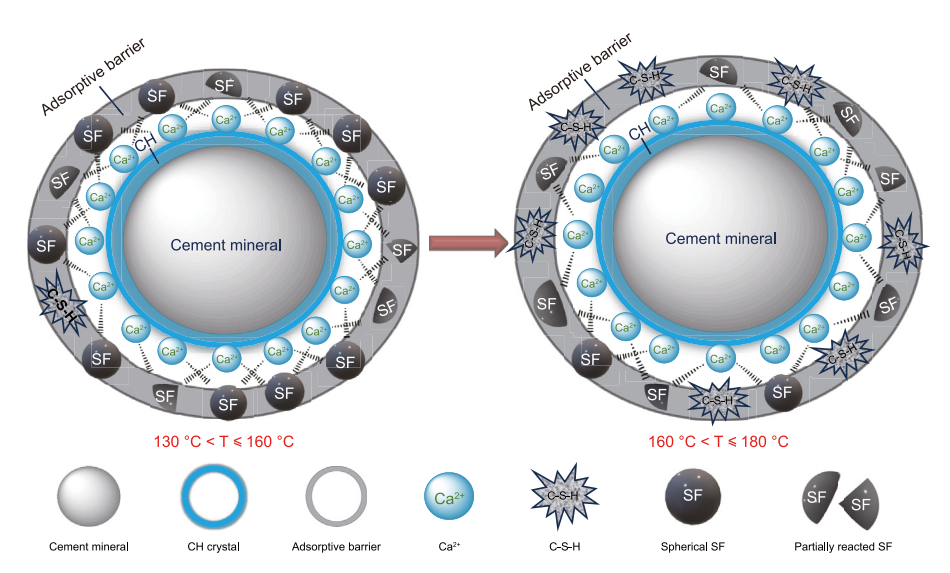


Fig. 14. Schematic diagram of the disappearance of "temperature-based TTR" and the occurrence of "dosage-based TTR" above 160 °C.

pozzolanic reaction efficiency and accelerated the generation of C-S-H so that led to the "dosage-based TTR".

As mentioned above, the "adsorptive barrier" effect enhanced with the increase of the temperature from 130 to 160 °C was the reason for the "temperature-based TTR". At 130–160 °C, both the pozzolanic reaction efficiency of SF and quartz sand were relatively low, and the effect of C–S–H on the TT was negligible. In contrast, the pozzolanic activity of the quartz sand and SF would get further reinforcement above 160 °C, correspondingly the generation rate of C–S–H increased. Therefore, the accelerated generation of C–S–H was the reason for the disappearance of the "temperature-based TTR" above 160 °C.

4. Conclusions and suggestions

In this work, the thickening progression mechanism of SF-OWC system at 130–180 $^{\circ}$ C was studied. Conclusions could be drawn as below:

- (1) The introduction of SF into OWC systems generally aggravated the bulging degree of the thickening curves and extended the TT above 130 °C, which induced the abnormal phenomena of "temperature-based TTR" between 130 and 160 °C and "dosage-based TTR" between 170 and 180 °C.
- (2) In the range of 130–160 °C, the TT of OWC slurry was positively correlated with the generation rate of CH crystal. The temperature rise shortened the TT and led to an accelerating accumulation of CH because of faster hydration as well as its decreased solubility. After adding SF, it covered the cement minerals' surface that were hydrating to produce CH driven by the pozzolanic reaction and its weak acid role, forming an "adsorptive barrier" to inhibit their further hydration and extend the TT. The enhanced "adsorptive barrier" effect from 130 to 160 °C was responsible for the "temperature-based TTR" phenomenon.
- (3) In the range of 170–180 °C, the TT of the OWC slurry was jointly controlled by the generation rate of CH and C–S–H because the generation rate of C–S–H significantly enhanced and exerted considerable impact on the thickening progression. Therefore, the accelerated generation of C–S–H was the reason for the disappearance of the "temperature-based TTR" above 160 °C. The OWC slurry without SF rapidly thickened at 1.26 h and produced a large amount of CH (8.08 wt%) and C–S–H (11.05 wt%) synchronously. The added SF could still play a dominant role in extending the TT due to the "adsorptive barrier" effect, but the TT shortened as SF dosages increased due to the fact that the pozzolanic reaction efficiency was promoted and the generation of C–S–H was accelerated, thereby the "dosage-based TTR" phenomenon was presented.

Based on the conclusions above, we suggest that the introduction of SF into the OWC slurry systems should be avoided if the cementing condition comprises the temperature range of $130-160~^{\circ}\text{C}$. Instead, biopolymers (welan gum, diutan gum, etc.) and clay minerals (diatomite, attapulgite, laponite, bentonite, etc) are preferred as alternatives of SF to regulate the suspension stability and the free fluid of OWC systems.

CRediT authorship contribution statement

Hang Zhang: Conceptualization, Formal analysis, Investigation, Methodology, Writing — original draft. **Miao-Miao Hu:** Data curation, Formal analysis, Methodology, Visualization, Writing — review

& editing. **Peng-Peng Li:** Formal analysis, Software, Supervision, Validation. **Guo-Qing Liu:** Formal analysis, Methodology, Software, Validation. **Qing-Lu Chang:** Formal analysis, Validation, Visualization. **Jie Cao:** Formal analysis, Investigation, Visualization. **Ming Liu:** Software, Validation. **Wen-Hua Xu:** Formal analysis, Resources, Supervision. **Xiu-Jian Xia:** Funding acquisition, Supervision, Validation. **Jin-Tang Guo:** Project administration, Resources, Supervision, Validation, Visualization, Writing — review & editing.

Acknowledgements

This work was supported by the Basic Research and Strategic Reserve Technology Research Fund Project of China National Petroleum Corporation (Grant No. 2021DQ03-14) and the National Natural Science Foundation of China (Grant No. 52204010). We also thank for the Haihe Laboratory of Sustainable Chemical Transformations for financial support.

Appendix A. Supplementary data

Supplementary data to this article can be found online at https://doi.org/10.1016/j.petsci.2023.12.025.

References

- API, 2013. API recommended Practice 10B-2. In: Recommended Practice for Testing Well Cements. American Petroleum Institute.
- Atiş, C.D., Özcan, F., Kılıç, A., et al., 2005. Influence of dry and wet curing conditions on compressive strength of silica fume concrete. Build. Environ. 40 (12), 1678–1683. https://doi.org/10.1016/j.buildenv.2004.12.005.
- Bhattacharya, M., Harish, K.V., 2018. An integrated approach for studying the hydration of portland cement systems containing silica fume. Construct. Build. Mater. 188, 1179—1192. https://doi.org/10.1016/j.conbuildmat.2018.08.114.
- Burroughs, J.F., Weiss, J., Haddock, J.E., 2019. Influence of high volumes of silica fume on the rheological behavior of oil well cement pastes. Construct. Build. Mater. 203, 401–407. https://doi.org/10.1016/j.conbuildmat.2019.01.027.
- Chakrabortya, A.K., Dutta, S.C., 2001. Study on silica fume modified mortar with various Indian cements cured at different temperatures. Build. Environ. 36, 375–382. https://doi.org/10.1016/S0360-1323(00)00017-2.
- Chen, D., Guo, J., Xia, X., et al., 2017. Abnormal gelation phenomenon of Class G oil well cement incorporating polycarboxylic additives and its countermeasures. Construct. Build. Mater. 149, 279–288. https://doi.org/10.1016/j.conbuildmat.2017.05.062.
- Cheng, X.W., Khorami, M., Shi, Y., et al., 2018. A new approach to improve mechanical properties and durability of low-density oil well cement composite reinforced by cellulose fibres in microstructural scale. Construct. Build. Mater. 177, 499–510. https://doi.org/10.1016/j.conbuildmat.2018.05.134.
- Diamond, S., Sahu, S., 2006. Densified silica fume: particle sizes and dispersion in concrete. Mater. Struct. 39 (9), 849–859. https://doi.org/10.1617/s11527-006-9087-y
- Greenberg, S.A., 1956. The chemisorption of calcium hydroxide by silica. J. Phys. Chem. 60 (3), 325–330. https://doi.org/10.1021/j150537a019.
- Guo, S., Bu, Y., Liu, H., et al., 2014. The abnormal phenomenon of class G oil well cement endangering the cementing security in the presence of retarder. Construct. Build. Mater. 54, 118–122. https://doi.org/10.1016/j.conbuildmat.2013.12.057.
- Guo, S., Bu, Y., Lu, Y., 2019a. Addition of tartaric acid to prevent delayed setting of oil-well cement containing retarder at high temperatures. J. Petrol. Sci. Eng. 172, 269–279. https://doi.org/10.1016/j.petrol.2018.09.053.
- Guo, S., Bu, Y., Zhou, A., et al., 2020. A three components thixotropic agent to enhance the thixotropic property of natural gas well cement at high temperatures. J. Nat. Gas Sci. Eng. 84, 103699. https://doi.org/10.1016/ j.jngse.2020.103699.
- Guo, S., Liu, H., Shan, Y., et al., 2017. The application of a combination of treated AMPS/IA copolymer and borax as the retarder of calcium aluminate phosphate cement. Construct. Build. Mater. 142, 51–58. https://doi.org/10.1016/ i.conbuildmat.2017.03.071.
- Guo, S., Zhang, Y., Wang, K., et al., 2019b. Delaying the hydration of Portland cement by sodium silicate: setting time and retarding mechanism. Construct. Build. Mater. 205, 543–548. https://doi.org/10.1016/j.conbuildmat.2019.02.041.
- Hakamy, A., Shaikh, F.U.A., Low, I.M., 2015. Characteristics of nanoclay and calcined nanoclay-cement nanocomposites. Compos. B Eng. 78, 174–184. https://doi.org/ 10.1016/j.compositesb.2015.03.074.
- Huang, C.Y., Feldman, R.F., 1985. Hydration reactions in portland cement-silica fume blends. Cement Concr. Res. 15, 585–592. https://doi.org/10.1016/0008-8846(85) 90056-0.
- Inan Sezer, G., 2012. Compressive strength and sulfate resistance of limestone and

or silica fume mortars. Construct. Build. Mater. 26 (1), 613–618. https://doi.org/10.1016/j.conbuildmat.2011.06.064.

- Jeong, Y., Kang, S.H., Kim, M.O., et al., 2020. Acceleration of cement hydration from supplementary cementitious materials: performance comparison between silica fume and hydrophobic silica. Cem. Concr. Compos. 112, 103688. https:// doi.org/10.1016/j.cemconcomp.2020.103688.
- Jiang, X., Song, Y., Duan, Z., 2008. Mechanism analyses of cement "high temperature reversal" caused by polyacrylamide. Drill. Fluid Complet. Fluid 25 (6), 47–49 (in Chinese)
- Jupe, A.C., Wilkinson, A.P., Luke, K., et al., 2008. Class H cement hydration at 180 °C and high pressure in the presence of added silica. Cement Concr. Res. 38 (5), 660–666, https://doi.org/10.1016/j.cemconres.2007.12.004.
- Kök, M.V., 2013. Thermal characterization of different origin class-G cements.

 J. Therm. Anal. Calorim. 115 (2), 1533–1539. https://doi.org/10.1007/s10973-013.3506-4
- Krakowiak, K.J., Thomas, J.J., Musso, S., et al., 2015. Nano-chemo-mechanical signature of conventional oil-well cement systems: effects of elevated temperature and curing time. Cement Concr. Res. 67, 103—121. https://doi.org/ 10.1016/j.cemconres.2014.08.008.
- Kurumisawa, K., Nawa, T., Owada, H., et al., 2013. Deteriorated hardened cement paste structure analyzed by XPS and ²⁹Si NMR techniques. Cement Concr. Res. 52, 190–195. https://doi.org/10.1016/j.cemconres.2013.07.003.
- Le Saout, G., Lécolier, E., Rivereau, A., et al., 2006. Chemical structure of cement aged at normal and elevated temperatures and pressures. Cement Concr. Res. 36 (1), 71–78. https://doi.org/10.1016/j.cemconres.2004.09.018.
- Lei, D.Y., Guo, L.P., Sun, W., et al., 2016. A new dispersing method on silica fume and its influence on the performance of cement-based materials. Construct. Build. Mater. 115, 716–726. https://doi.org/10.1016/j.conbuildmat.2016.04.023.
- Li, B., Gao, A., Li, Y., et al., 2023a. Effect of silica fume content on the mechanical strengths, compressive stress-strain behavior and microstructures of geopolymeric recycled aggregate concrete. Construct. Build. Mater. 384, 131417. https://doi.org/10.1016/j.conbuildmat.2023.131417.
- Li, P., Hu, M., Liu, M., et al., 2022. Thixotropic and hydration effects of Mg/Al-layered double hydroxide and sodium montmorillonite composite dispersion on oil well cement paste. Cem. Concr. Compos. 134, 104785. https://doi.org/10.1016/ j.cemconcomp.2022.104785.
- Li, P., Hu, M., Liu, M., et al., 2023b. Regulation of oil well cement paste properties by nanoclay: rheology, suspension stability and hydration process. Construct. Build. Mater. 377, 131049. https://doi.org/10.1016/j.conbuildmat.2023.131049.
- Li, S., 2020. Study and application of an ultra-low-density cement slurry. Drill. Fluid Complet. Fluid 37 (5), 644–650. https://doi.org/10.3969/j.issn.1001-5620.2020.05.018.
- Liu, H., Bu, Y., Sanjayan, J., et al., 2015. Effects of chitosan treatment on strength and thickening properties of oil well cement. Construct. Build. Mater. 75, 404–414. https://doi.org/10.1016/j.conbuildmat.2014.11.047.
- Liu, H., Pang, X., Santra, A., et al., 2023. Editorial: advances in wellbore servicing fluids and materials. Frontiers in Materials 9. https://doi.org/10.3389/ fmats.2022.1118773.
- Liu, Q., Lu, Z., Hu, X., et al., 2021. A mechanical strong polymer-cement composite fabricated by in situ polymerization within the cement matrix. J. Build. Eng. 42, 103048. https://doi.org/10.1016/ji.jobe.2021.103048.
- Lu, Y., Li, M., Guo, Z., et al., 2016. A novel high temperature retarder applied to a long cementing interval. RSC Adv. 6 (17), 14421–14426. https://doi.org/10.1039/ c5ra24638e.
- Mendes, A., Gates, W.P., Sanjayan, J.G., et al., 2011. NMR, XRD, IR and synchrotron NEXAFS spectroscopic studies of OPC and OPC/slag cement paste hydrates. Mater. Struct. 44 (10), 1773—1791. https://doi.org/10.1617/s11527-011-9737-6.
- Mitchell, D.R.G., Hinczak, I., Day, R.A., 1998. Interaction of silica fume with calcium hydroxide solutions and hydrated cement pastes. Cement Concr. Res. 28 (11), 1571–1574. https://doi.org/10.1016/S0008-8846(98)00133-1.
- Pang, X., Sun, L., Chen, M., et al., 2022. Influence of curing temperature on the hydration and strength development of Class G Portland cement. Cement Concr. Res. 156, 106776. https://doi.org/10.1016/j.cemconres.2022.106776.
- Peng, Z., Chen, C., Feng, Q., et al., 2020. Synthesis and characterization of a quaternary copolymer retarder for cementing in a long sealing section with large

- temperature difference. New J. Chem. 44 (9), 3771–3776. https://doi.org/10.1039/c9ni06150a.
- Pernites, R.B., Santra, A.K., 2016. Portland cement solutions for ultra-high temperature wellbore applications. Cem. Concr. Compos. 72, 89–103. https://doi.org/10.1016/j.cemconcomp.2016.05.018.
- Qian, X.Q., Qian, K.L., Meng, T., et al., 2008. Effect of mineral admixtures, nano-SiO₂ and nano-CaCO₃ on water demand of cement paste. Rare Met. Mater. Eng. 37, 709–711. https://doi.org/10.1002/pip.801.
- Qin, J., Pang, X., Cheng, G., et al., 2021. Influences of different admixtures on the properties of oil well cement systems at HPHT conditions. Cem. Concr. Compos. 123, 104202. https://doi.org/10.1016/i.cemconcomp.2021.104202.
- Romano, R.C.d.O., Bernardo, H.M., Maciel, M.H., et al., 2019. Using isothermal calorimetry, X-ray diffraction, thermogravimetry and FTIR to monitor the hydration reaction of Portland cements associated with red mud as a supplementary material. J. Therm. Anal. Calorim. 137 (6), 1877–1890. https://doi.org/ 10.1007/s10973-019-08095-x.
- Scheinherrová, L., Trník, A., Pokorný, J., et al., 2017. Effect of silica fume on hydration of air-cured blended cement pastes measured by DSC/TG analysis. AIP Conf. Proc. 1863 (150009). https://doi.org/10.1063/1.4992331.
- Shannag, M.J., 2000. High strength concrete containing natural pozzolan and silica fume. Cem. Concr. Compos. 22 (6), 399–406. https://doi.org/10.1016/S0958-9465(00)00037-8.
- Sharma, U., Singh, L.P., Zhan, B., et al., 2019. Effect of particle size of nanosilica on microstructure of C–S–H and its impact on mechanical strength. Cem. Concr. Compos. 97, 312–321. https://doi.org/10.1016/j.cemconcomp.2019.01.007.
- Sun, F., Pang, X., Kawashima, S., et al., 2022. Effect of tartaric acid on the hydration of oil well cement at elevated temperatures between 60 °C and 89 °C. Cement Concr. Res. 161, 106952. https://doi.org/10.1016/j.cemconres.2022.106952.
- Sun, L.J., Pang, X.Y., Ghabezloo, S., et al., 2023a. Modeling the hydration, viscosity and ultrasonic property evolution of class G cement up to 90 °C and 200 MPa by a scale factor method. Petrol. Sci. 20 (4), 2372–2385. https://doi.org/10.1016/ i.petsci.2023.01.014.
- Sun, L., Pang, X., Ghabezloo, S., et al., 2023b. Hydration kinetics and strength retrogression mechanism of silica-cement systems in the temperature range of 110 °C–200 °C. Cement Concr. Res. 167, 107120. https://doi.org/10.1016/j.cemconres.2023.107120.
- Vikan, H., Justnes, H., 2007. Rheology of cementitious paste with silica fume or limestone. Cement Concr. Res. 37 (11), 1512–1517. https://doi.org/10.1016/ j.cemconres.2007.08.012.
- Vuk, T., Ljubic-Mlakar, T., Gabrovsek, R., et al., 2000. Tertiary gelation of oilwell cement. Cement Concr. Res. 30 (11), 1709—1713. https://doi.org/10.1016/S0008-8846(00)00414-2.
- Wang, C., Wang, L., Geng, C., et al., 2022a. Benefits of delayed addition of rutin on the thickening time and compressive strength of oil well cement. Construct. Build. Mater. 322, 126287. https://doi.org/10.1016/j.conbuildmat.2021.126287.
- Wang, C., Wang, L., Yao, X., et al., 2022b. The effect of rutin on the early-age hydration of oil well cement at varying temperatures. Cem. Concr. Compos. 128, 104438. https://doi.org/10.1016/j.cemconcomp.2022.104438.
- Yajun, J., Cahyadi, J.H., 2003. Effects of densified silica fume on microstructure and compressive strength of blended cement pastes. Cement Concr. Res. 33 (10), 1543–1548. https://doi.org/10.1016/s0008-8846(03)00100-5.
- Yang, R., He, T., 2021. Influence of liquid accelerators combined with mineral admixtures on early hydration of cement pastes. Construct. Build. Mater. 295, 123659. https://doi.org/10.1016/j.conbuildmat.2021.123659.
- Zhang, H., Hu, M., Li, P., et al., 2023. Covalently bonded AMPS-based copolymer C S H hybrid as a fluid loss additive for oilwell saline cement slurry in UHT environment. Construct. Build. Mater. 378, 131199. https://doi.org/10.1016/j.conbuildmat.2023.131177.
- Zhang, H., Hu, M., Xu, Y., et al., 2021. Inhibitory effects of functionalized polycarboxylate retarder on aberrant thickening phenomena of oil well cement at high temperature. Construct. Build. Mater. 274, 121994. https://doi.org/10.1016/ j.conbuildmat.2020.121994.
- Zhang, Z., Zhang, B., Yan, P., 2016. Comparative study of effect of raw and densified silica fume in the paste, mortar and concrete. Construct. Build. Mater. 105, 82–93. https://doi.org/10.1016/j.conbuildmat.2015.12.045.